J Appl Electrochem (2013) 43:43–51
DOI 10.1007/s10800-012-0503-4

ORIGINAL PAPER

Electrochemical behavior of nanostructured nickel phthalocyanine (NiPc/C) for oxygen reduction reaction in alkaline media

Lei Ding · Qing Xin · Xuejun Zhou · Jinli Qiao · Hui Li · Haijang Wang

Received: 23 June 2012 / Accepted: 29 October 2012 / Published online: 8 November 2012

Abstract Carbon-supported nickel phthalocyanine (NiPc/C) nanoparticle catalysts have been synthesized by a simple solvent-impregnation and milling procedure, then heat-treated at 600, 700, 800 and 900 °C to optimize their activity for the oxygen reduction reaction (ORR). The electrocatalytic activity and electron transfer mechanism of NiPc/C catalysts were demonstrated in oxygen-saturated alkaline electrolyte by cyclic voltammetry, linear sweep voltammetry as well as rotating disk electrode techniques, respectively. The results show that the heat-treatment temperature has a remarkable impact on the ORR activity of NiPc/C. An onset potential of 0.05 V and a half-wave potential of −0.15 V are achieved in 0.1 M KOH after the catalyst was heat-treated at 800 °C. In addition to an increase in ORR kinetics, the number of electrons transferred for ORR also increased from 2.2 to 2.8 with increasing heat-treatment temperature from 600 to 800 °C. To understand the heat-treatment effect, X-ray diffraction, transmission electron microscopy, thermogravimetric analysis, and X-ray photoelectron spectroscopy (XPS) were used to identify the catalyst structure and composition. From XPS analysis, pyridinic-N and graphitic-N were clearly observed after the sample was heat-treated at 800 °C. Both of these species might be assigned to sites catalytically active toward the ORR leading to activity enhancement.

Keywords Nickel phthalocyanine · Oxygen reduction reaction · Heat-treatment · Polymer electrolyte membrane fuel cell

1 Introduction

Proton-exchange membrane (PEM) fuel cells as efficient energy conversion devices have been considered one of the most promising clean powder sources [1, 2]. However, despite over a century of study and decades of intensive research, the cost of PEM fuel cells still inhibits its large-scale commercialization. Recently, alkaline fuel cells (AFC) have appeared to be the most promising power source on a cost basis [3–5]. This kind of fuel cell uses an alkaline electrolyte, where the oxygen reduction reaction (ORR) is much faster than in the acidic media for PEM fuel cells. The faster ORR kinetics in alkaline media makes it possible to use non-Pt catalysts to achieve the desirable kinetics for ORR and, the high stability of the electrode material afforded. In addition, the use of non-Pt catalysts can effectively reduce the cost of the fuel cell system [6, 7].

Due to the advantages associated with alkaline fuel cell systems, significant interests have been evoked on the development of non-Pt catalysts including various transition metals and macrocyclic complexes [8, 9]. Among these catalysts, heat-treated metal-N_4 macrocycles (MN4), such as phthalocyanine (MPc) complexes and porphyrins, have been considered the most promising ORR catalysts because of their conjugated structure and good chemical stability [10–13].

L. Ding · Q. Xin · X. Zhou · J. Qiao (✉)
College of Environmental Science and Engineering, Donghua University, 2999 Ren'min North Road, Shanghai 201620, People's Republic of China
e-mail: qiaojinli@hotmail.com; qiaojl@dhu.edu.cn

Q. Xin · X. Zhou · H. Li · H. Wang (✉)
Institute for Fuel Cell Innovation, National Research Council Canada, 4250 Wesbrook Mall, Vancouver, BC V6T 1W5, Canada
e-mail: haijiang.wang@nrc.gc.ca

For pyrolyzed transition metal macrocycle catalysts, it has been reported that four ingredients are required to make well-performing ORR catalysts that exhibit both ORR catalytic activity and stability: transition metal, nitrogen coordinators on these catalysts, carbon support, and the process of pyrolysis [14]. With respect to transition metal, macrocycles with different transition metals may display diverse activities, and the electrocatalytic activity of various transition metals follows the order: $Fe^{2+} > Co^{2+} > Mn^{2+} > Ni^{2+}$, Cu^{2+} [15]. Co- and Fe-centered phthalocyanines are thus popular non-noble metal catalysts that have attracted significant efforts due to their reasonable activity and remarkable selectivity toward ORR in both acidic and alkaline electrolytes [16–20]. Nevertheless, little attention has been given to other metal-centered phthalocyanines in the past decades because of the fact that, in strong acidic conditions, such as in PEM fuel cell operating conditions, both activity and stability are much more difficult to achieve. For example, Ozaki et al. [21] reported a procedure to prepare the ORR catalysts using Li- and Mg-phthalocyanines as nitrogen-doping agents, but their ORR activities are much lower than those of Co- and Fe-centered phthalocyanines. Most recently, Sehlotho and Nyokong [22] measured the ORR activity of several types of Mn–phthalocyanine complexes tetra-substituted with different peripheral ligands. By changing the pH value of solution from 1 to 12, they found that the electron transfer number per oxygen molecule in the overall reduction process was $2e^-$ in acidic or slightly alkaline media, but $4e^-$ in alkaline media.

In view of these facts, we speculated that other metal-centered phthalocyanines could show high catalytic activity toward ORR when changing the electrolyte from acidic to alkaline. Up to now, there is no report on the carbon-supported Ni-centered phthalocyanine as electrochemical catalyst for alkaline fuel cell studies, except for our work [23]. In this study, carbon-supported nickel phthalocyanines (NiPc/C) as a typical target was studied as cathode catalyst after heat-treatment. Both electrochemical measurements and physical characterization were performed to study its electrocatalytic activity and its structure and morphology. In case of electrochemical measurements, cyclic voltammetry (CV), and linear sweep voltammetry (LSV) techniques were employed to investigate the electrocatalytic activity of NiPc/C heat-treated at different temperatures. RDE theory was used to clarify the ORR mechanisms of NiPc/C with increasing the heat-treatment temperature. With respect to physical characterization, transmission electron microscopy (TEM), and X-ray diffraction (XRD) and TG were conducted to determine the structure and morphology of NiPc/C at different temperatures. In addition, XPS was used to detect surface structure changes and shed some light on the nature of the active centers of the catalyst.

2 Experimental

2.1 Materials and catalyst preparation

Nickel phthalocyanine (NiPc) was purchased from Sigma-Aldrich with 97 % purity and used as-received without further purifications. Carbon Black (Vulcan XC-72, 254 $m^2\ g^{-1}$) was purchased from Cabot Corporation and used as support for all catalysts. In order to disperse the catalysts on the surface of carbon black, 0.4 g NiPc and 0.6 g Vulcan XC-72 were mixed with 100-ml ethanol under constant milling in a mortar for about 2 h to obtain a uniform mixture. This mixture was then dried in vacuum at 40 °C for about 1 h to remove ethanol. After drying, the resulting powder was heat-treated at 600, 700, 800, and 900 °C for 120 min under N_2 atmosphere, respectively. For convenience, the catalysts heat-treated at different temperatures were denoted as NiPc/C-600, NiPc/C-700, NiPc/C-800, and NiPc/C-900, respectively. H_2Pc/C as a reference was also synthesized using the same procedure.

2.2 Physical characterization

TG analyses were carried out on a NETZSCH simultaneous thermal analyzer TG 209. Catalysts samples of about 10 mg were loaded into an alumina pan, and then heated from 25 to 900 °C at a rate of 10 °C min^{-1}. All measurements were conducted under nitrogen. The vacant alumina pan was used as a reference throughout the whole experiments.

The crystal-phase XRD patterns were collected on a Philips PW3830 X-ray diffractometer using Cu-Kα radiation ($\lambda = 0.15406$ nm). The current was 40 mA and the voltage was 40 kV. The intensity data were collected at 25 °C in the 2θ range from 5° to 90° with a scan rate of 1.20° min^{-1}.

TEM analyses were performed on a high-resolution Hitachi JEM-2100F operating at 200 kV to obtain information of the average particle size and the size distribution of the catalysts prepared.

XPS analysis was conducted using a Kratos AXIS $Ultra^{DLD}$ electron spectrometer to determine the surface composition with Al K X-ray anode source ($hv =$ 1486.6 eV) at 250 W and 14.0 kV.

2.3 Electrochemical measurements

Electrochemical measurements were conducted through CV and LSV techniques using a potentiostat CHI 760 electrochemical analyzer. A conventional three-compartment electrochemical cell was employed for all electrochemical tests, in which a saturated calomel electrode (SCE) was used as the reference electrode and a platinum foil was used

as the counter electrode. A rotating disk electrode (RDE) made of glassy carbon (GC) electrode with a diameter of 6.0 mm (corresponding to a geometric surface area of 0.283 cm^2, Pine, 5908Triangle Drive, Raleigh, NC) was used as the working electrode, on which a layer of the studied catalysts was casted. The working electrode was coated with catalysts using the following steps: 4 mg of the NiPc/C catalyst was suspended in 2 ml of methanol/Nafion® solution (50:1 in mass) to form a catalyst ink, which was ultrasonically dispersed for 10 min. Then, 10 µl of the suspension was pipetted onto the surface of GC electrode and then dried at room temperature for testing. The catalyst loading of each electrode was 70.6 µg cm^{-2}. All measured potentials were converted into the values referring to a standard hydrogen electrode (SHE).

RDE measurements were performed in 0.1 M KOH solution at room temperature. For every test, CV was first carried out by scanning the disk potential from −0.3 to 0.6 V at a scan rate of 50 mV s^{-1} to examine the surface behavior of the catalyst in N_2-saturated 0.1 M KOH solution. Then O_2 was bubbled into the solution to form an O_2-saturated solution for ORR measurement. For more quantitative measurements of ORR activity of the catalysts, LSV was performed in the potential range between −0.7 and 0.2 V in O_2-saturated 0.1 M KOH solution at desired rotating rate. In order to ensure a steady state at each point of the LSV curves, a slow sweeping rate of 5 mV s^{-1} was applied.

3 Results and discussion

3.1 Electrochemical activity of NiPc/C catalysts toward ORR

Although the catalyzed ORR mechanisms of MPc catalysts are still not fully understood, there has been a general agreement in the literature that heat treatment can effectively improve the electrocatalytic activity of the catalysts [24, 25]. In order to pursue the best catalytic performance for ORR, the influence of heat treatment on the catalytic activity of NiPc/C catalysts was investigated by CV and LSV. Figure 1 shows the CV curves of N_2- and O_2-saturated 0.1 M KOH solution obtained with the GC electrode coated with NiPc/C catalysts. It can be seen that there is no reduction peaks of oxygen at the NiPc/C catalyst electrodes in N_2-saturated 0.1 M KOH solution. However, clear reduction peaks are observed in O_2-saturated 0.1 M KOH solution for all NiPc/C catalysts after heat treatment at various temperatures: −0.21 V for NiPc/C-600, −0.17 V for NiPc/C-700, −0.15 V for NiPc/C-800, and −0.17 V for NiPc/C-900. In addition, the ORR peak current density changes with increasing the heat-treatment temperature and reaches a maximum value at 800 °C. Among all the curves in Fig. 1, there is no peak attributed to the $Ni^{3+/2+}$ redox, which indicates that the element nickel is in some other state, rather than nickel ions adsorbed on the carbon surface.

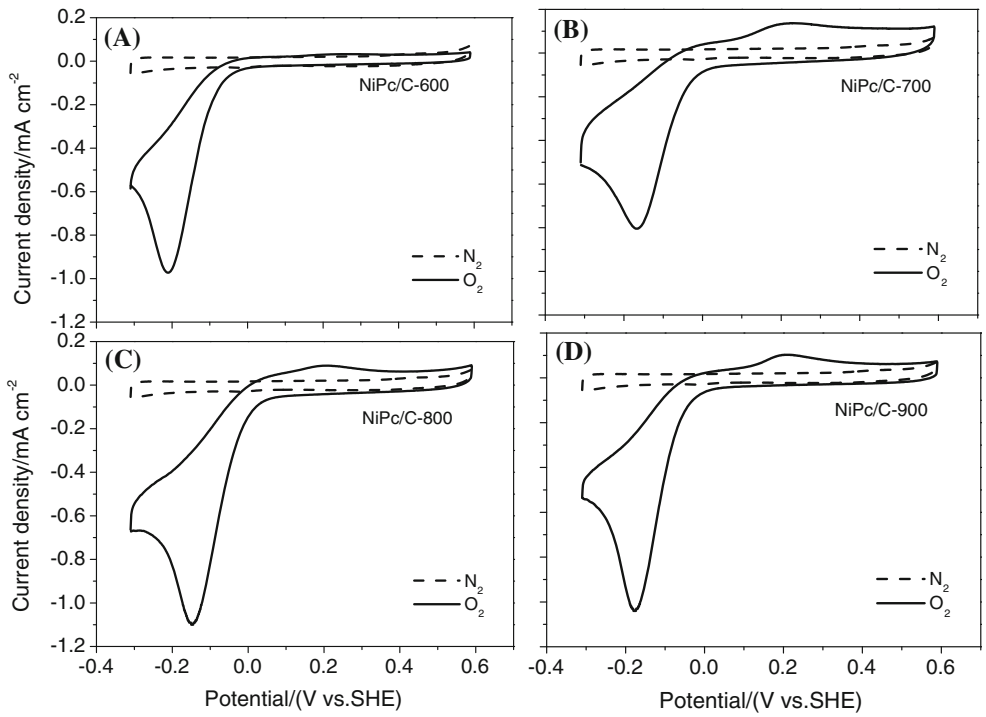

Fig. 1 Cyclic voltammograms of NiPc/C catalysts heat-treated at different temperatures in N_2-saturated and O_2-saturated 0.1 M KOH at room temperature. Scan rate: 50 mV s^{-1}

In order to investigate the eletrocatalytic activity of NiPc/C catalysts for the ORR after heat treatment at different temperatures, LSV was carried out using RDE technique after GC electrodes coated with NiPc/C catalysts heat-treated at 600, 700, 800, and 900 °C, respectively, and the polarization curves obtained are shown in Fig. 2A. It can be seen that for catalyst samples heat-treated at 600, 700, and 900 °C, the onset potentials for the ORR are all located near 0.03 V, which are lower than that of the sample heat-treated at 800 °C (near 0.05 V). The same trend can also be observed in the half-wave potentials of the catalysts, which are NiPc/C-800 (−0.15 V) > NiPc/C-700 ≈ NiPc/C-900 (−0.17 V) > NiPc/C-600 (−0.21 V), suggesting that ~800 °C may be the optimal temperature in obtaining the most active electrocatalyst for the ORR.

To further verify the heat-treatment temperature effect on the ORR activity, the current densities at −0.15, −0.10, and −0.05 V are plotted as the function of temperatures and, the results are shown in Fig. 2B. As can be seen, the current density increases significantly with increasing the heat-treatment temperature from 600 to 800 °C. Above 800 °C, the current density decreases again and shows the lowest value when the heat-treatment temperature for the catalyst synthesis is at 900 °C. The phenomenon clearly indicates that below 800 °C, more ORR active sites in the NiPc/C catalyst could be produced. While, when temperature is high enough such as at 900 °C, a portion of the active sites may be damaged to form other structures, such as metallic nickel or nickel carbide, which are less active for the ORR. These will be discussed thoroughly below. According to the curves shown in Fig. 2B, we can conclude that the optimal heat-treatment temperature is around 800 °C. Therefore, in the subsequent study the NiPc/C obtained at 800 °C was selected as the target catalyst.

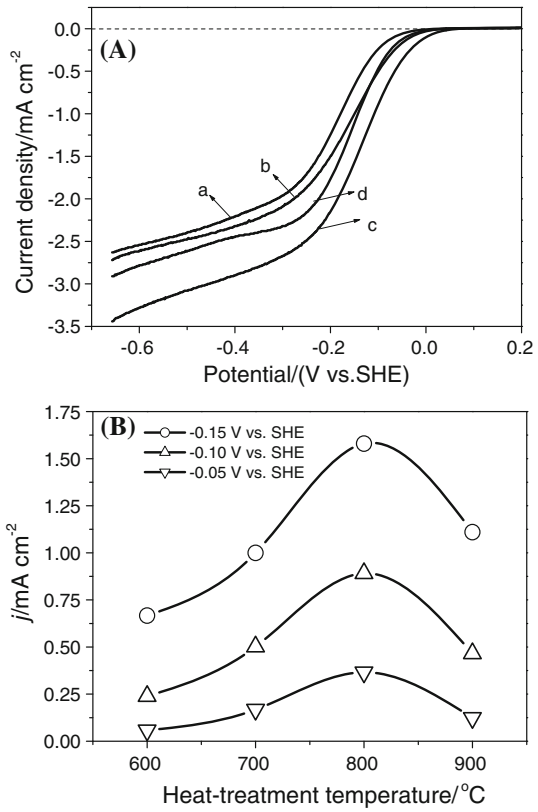

Fig. 2 **A** Current–voltage curves for ORR catalyzed by NiPc/C catalysts heat-treated at (*a*) 600 °C, (*b*) 700 °C, (*c*) 800 °C and (*d*) 900 °C measured in O_2-saturated 0.1 M KOH at the scan rate 5 mV s^{-1}. Electrode rotating rate: 1,500 rpm. **B** Current densities at −0.05, −0.10 and −0.15 V versus SHE as a function of catalyst heat-treatment temperature with data obtained from (**A**)

3.2 Kinetic study of the ORR catalyzed by heat-treatment NiPc/C

The kinetics of ORR catalyzed by NiPc/C in alkaline media was studied by LSV at various rotation rates, which were processed using the Koutecky–Levich (K–L) equations [26]:

$$i_k = i \cdot i_d/(i_d - i) \quad (1)$$

$$i_i = B\omega^{1/2} \quad (2)$$

$$B = 0.2nFSCo_2Do_2^{2/3}v^{-1/6} \quad (3)$$

where B is the Levich slope, ω is the rotation rate, n is the electron transfer number per oxygen molecule, F is Faraday constant, S the electrode geometric surface area, C_O is the concentration of oxygen, D_O is the diffusion coefficient of O_2 in the electrolyte, v is the kinetic viscosity and the constant 0.2 is adopted when rotation speed is expressed in revolutions per minute. Figure 3A shows the polarization curves at various rotation rates for ORR on the GC electrode coated with NiPc/C-800 in O_2-saturated 0.1 M KOH solution as a typical candidate. It can be seen that the limiting current for ORR increases with the rotation rate, while the onset potential of the catalyst for ORR remains unchanged. Figure 3B shows K–L plot at −0.6 V for NiPc/C-800, which indicates the estimation of overall electron number (n) transferred per oxygen molecule. For a better comparison, K–L plots of NiPc/C catalysts heat-treated at other temperatures are also depicted in Fig. 3B. From the slopes of the K–L plots, the electron transfer numbers per oxygen molecule in the overall reduction process can be calculated, and it was found that the n values change with increasing the heat-treatment temperature: 2.23 for NiPc/C-600, 2.15 for NiPc/C-700, 2.93 for NiPc/C-800, and 2.38 for NiPc/C-900. These data suggest that the ORR catalyzed on NiPc/C-600, NiPc/C-700, and NiPc/C-900 electrodes is mainly a $2e^-$ reduction process leading to a large amount of H_2O_2. However, for NiPc/C-800 electrode, the electron

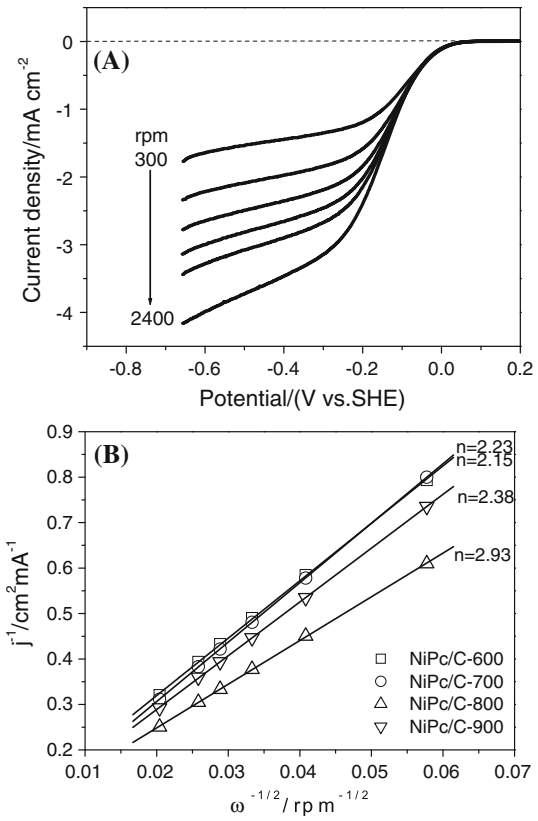

Fig. 3 **A** Current–voltage curves at various electrode rotating rates obtained with NiPc/C-800 catalyst in O_2-saturated 0.1 M KOH at the scan rate 5 mV s^{-1}. **B** Koutecky–Levich plots for the ORR at −0.6 V versus SHE from the current–voltage curves recorded at the same conditions as those in (**A**) using catalysts obtained at various heat-treatment temperatures

transfer number is 2.93, which lies between the $2e^-$ and $4e^-$ reduction process, suggesting a great effect on the decreasing of H_2O_2 by heat treatment at 800 °C. It should be mentioned that compared to other metal centers, Fe- and Co-centered macrocyclic complexes exhibit the highest activity no matter in acid or alkaline media [17, 18]. For example, Chen et al. reported that onset potentials for ORR on the CoPc/C and FePc/C were −0.05 and 0.05 V versus Hg/HgO, respectively. Then, the half-wave potentials were around −0.12 V versus Hg/HgO on the CoPc/C, −0.05 V versus Hg/HgO on the FePc/C [17]. It can be seen that the catalytic activity of NiPc/C-800 prepared in this study is much higher than that of the NiPc/C-600, NiPc/C-700, and NiPc/C-900 catalysts, it is still lower than Co- and Fe-centered phthalocyanines. However, the production of amount of H_2O_2 is hindered on NiPc/C-800 in comparison with the cases on CoPc/C [17].

It has been identified that ORR catalytic activity and selectivity of metal phthalocyanines require a carbon support, a source of metal and N, and thermal treatment at appropriate temperatures [20]. Therefore, optimizing these experiment conditions to reach optimum activity and selectivity of NiPc/C will be our next research. For instance, in our recent study, we have prepared CoPc/C modified with Fe as co-added catalyst. The results showed that the catalytic activity CoPc/C is greatly improved with 5 % Fe loading, which was demonstrated by the observed positive shift more than 70 mV for the onset potential and near 30 mV for the half-wave potential [27]. Kruusenberg et al. have synthesized Co- and Fe-centered phthalocyanine catalysts using multi-walled carbon nanotubes. The electrochemical test showed that CoPc/MWCNTs and FePc/MWCNTs are more active toward the ORR than these catalysts prepared by Vulcan XC-72 carbon support. The fuel cell tests performed almost similar to that of E-TEK catalyst [28].

3.3 Studies on the active site structures of the NiPc/C catalysts

Figure 4 shows the TG and the DTG curves for H_2Pc/C and NiPc/C, respectively. As shown in Fig. 4A, H_2Pc/C shows only one major peak at 550 °C with a weight loss of about 30 wt%, indicative of the decomposition of H_2Pc [19]. In the case of NiPc/C, situations are different. The DTG curve of NiPc/C shows three peaks at around 150, 560, and 760 °C, respectively (Fig. 4B). Corresponding to DTG, there are three steps on the curve of TG. (1) The first step starts at 130 °C to reach a plateau near 250 °C with a

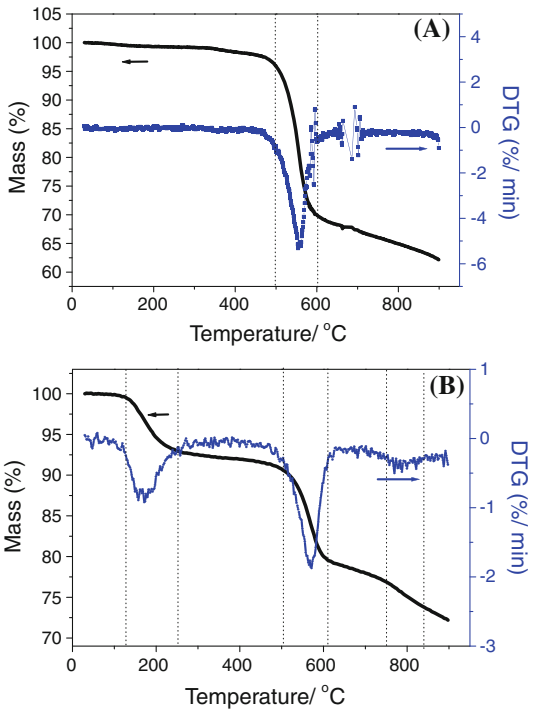

Fig. 4 TG/DTG curves of **A** H_2Pc/C and **B** NiPc/C

weight loss of about 7.5 wt%. In this stage, NiPc has a stable molecular structure and, a small amount of weight loss due to volatilization of absolute ethanol and water molecules. (2) The second step starts at 500 °C and ends at 610 °C with 10.5 wt% weight loss, which may correspond to the thermal decomposition of the phthalocyanine. (3) The decomposition of NiPc/C chelate happens at a temperature above 610 °C. This step corresponds to the pyrolysis of the carbonaceous compounds (whether Vulcan char or deposited phthalocyanine). Note that the catalytic activities of NiPc/C-700, NiPc/C-800, and NiPc/C-900 are all much higher than that of the NiPc/C-600. This suggests that catalytic active sites are probably formed at the third step. Furthermore, the total mass loss of NiPc/C is smaller than that of the H_2Pc/C by about 12 %. As seen in Fig. 4, H_2Pc/C shows only one H_2Pc decomposition process, whereas NiPc/C shows two NiPc decomposition processes, which indicate that decomposition rate of NiPc/C is much slower than that of the H_2Pc/C catalyst. In other words, the decomposition stage is hindered greatly for NiPc/C. Vallejos-Burgos et al. [24] also found that central coordinating metal gives phthalocyanine structure a higher thermal stability. All this implies that Ni species may prevent phthalocyanine from thermal decomposition and lead to higher stability which are helpful to form more ORR activity sites as discussed in the following section.

XRD analyses were conducted to obtain crystallographic information on the NiPc/C catalysts. Figure 5 shows the XRD patterns of NiPc/C catalysts after heat treatment at 600, 700, 800, and 900 °C, respectively. The first large broad peak located at about $2\theta = 25°$ in all the XRD patterns can be assigned to the strong graphite character of the Vulcan XC-72. For catalyst sample heat treated at 600 °C, it shows only one peak at 44.5°, which is assigned to the Ni (111) peak. This weak peak indicates that the structure of NiPc starts to decompose. When heat-treatment temperature is increased from 700 to 900 °C, two

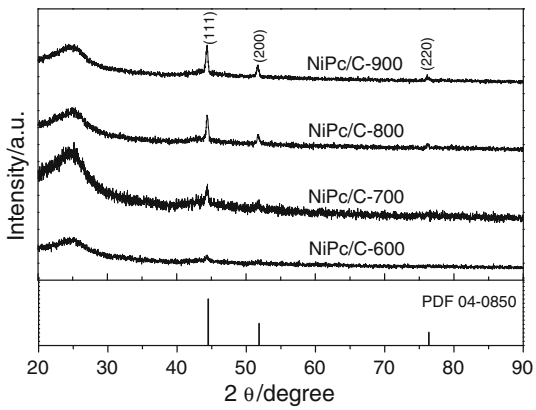

Fig. 5 XRD patterns of NiPc/C catalysts heat-treated at 600, 700, 800, and 900 °C, respectively

new diffraction peaks at 51.8° and 76.3° appeared, indicating that the decomposition of NiPc/C structure is more deeper than that of 600 °C during the heat-treatment process and the aggregation of metallic nickel occur at higher temperature. These two peaks centered at 51.8° and 76.3° are corresponding to the Ni (200) peak and Ni (220) peak, and these two peaks become sharpened with the increase in heat-treatment temperature, which suggests that Ni clusters grow at higher pyrolyzing temperature.

Another confirmation of the presence of metallic Ni in the NiPc/C catalysts heat-treated at different temperatures can be seen from Fig. 6, in which TEM images of the NiPc/C obtained at 600, 700, 800, and 900 °C heat treatment are illustrated. It can be seen that some Ni metal particles appear but without a clear shape after heat treatment at 600 °C. What is more, some aggregates can be observed with an average particle size of 50 nm on the carbon support surface (Fig. 6A). When the catalyst is heat-treated at 700 °C, the aggregation increases, and some smaller size of the particle clusters are observed with the size ranging from 10 to 20 nm (Fig. 6B). With further increasing the temperature to 800 °C, the existence of metal particles with an average particle size of 30 nm is clearly observed, which are uniformly dispersed on the Vulcan XC-72 support (Fig. 6C, inset). However, with further increasing the temperature to 900 °C, both small (with an average particle size of 20 nm) and large particles (with an average particle size of 70 nm) can be observed (Fig. 6D, inset). The NiPc/C is in a highly crystalline phase (the Ni crystallites growth) after high-temperature treatment. These results suggest that heat treatment can decompose the NiPc/C to metallic Ni, which then agglomerates into large particles when the heat-treatment temperature is increased. This result is in agreement with the observations from the XRD analysis in Fig. 5. In general, metallic Ni is not active for the ORR. Hence, to prevent the formation of metallic Ni in the catalyst, the heat treatment should be conducted not at a too high temperature. As shown in Fig. 2, NiPc/C catalyst sample heat-treated at 800 °C shows the best ORR activity, indicating that a lot of active sites may forms at this temperature, although some small metallic Ni particles are observed. In order to gain some information on active sites of the catalysts as-prepared, the surface characterization of NiPc/C catalysts after heat-treatment at 800 °C was carried out by XPS.

Figure 7 shows the N 1s spectral region for NiPc/C-800 as an typical candidate, where the N signal is divided into four bands, marked N_I, N_{II}, N_{III}, and N_{IV}. The N_I band at lower binding energy of 398.8 eV could be assigned to pyridinic-N, the N_{II} band at 399.9 eV, and the N_{III} band at 401.2 eV may be related to pyrrolic-N and graphitic-N. Finally, the broader N_{IV} band at 404.3 eV could be attributed to N–O bonds (pyridine-N-oxide) [21, 29–33]. According to the literatures, pyridine-N and graphitic-N are

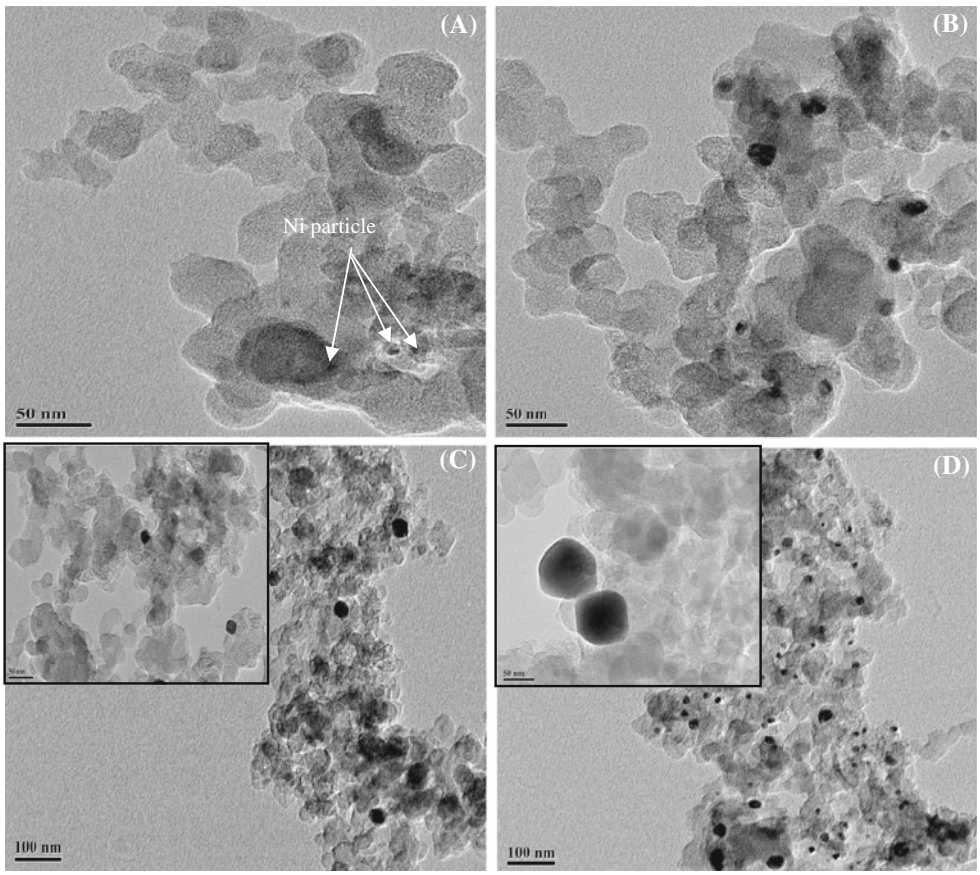

Fig. 6 TEM images for NiPc/C catalyst heat-treated at **A** 600 °C, **B** 700 °C, **C** 800 °C, and **D** 900 °C

believed to play an important roles in determining the electrocatalytic ORR activity and stability of macrocycles, while pyridine-N-oxide seems useless in improving the activity [34, 35]. In the case of NiPc/C-800, it can be clearly seen that both pyridinic-N and graphitic-N are the major bands in this sample forming the ORR active sites, although pyridine-N-oxide can also be observed. Similar results are observed in our recent study as for CuPc/C [36]. Sidik et al.

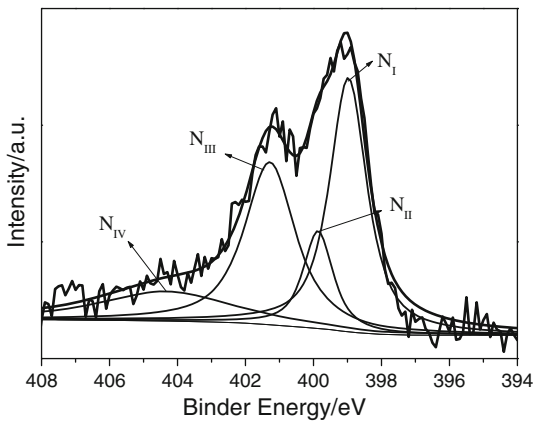

Fig. 7 XPS spectra in the N 1s region for the NiPc/C catalysts heat-treated at 800 °C

[37] once observed that graphitic-N could catalyze the ORR through a $4e^-$ pathway. That is why we observed the high ORR activity catalyzed by NiPc/C-800 catalyst. This study may at least partially explain the results that the electron transfer number of NiPc/C-800 is higher than NiPc/C catalysts heat-treated at other temperatures. Therefore, it can be concluded that both pyridinic-N and graphitic-N bonded by Ni ions should be mainly responsible for the enhanced ORR activity in this study [36]. According to the literatures [32–35, 38], MN_2/C represents a metal ion coordinating to two nitrogen atoms of the pyridinic type, while MN_4/C stands for a metal ion coordinating to four nitrogen atoms of the pyrrolic type. Therefore, we can speculate that the NiN_4/C and NiN_2/C coexist in NiPc/C catalysts after the sample was heat-treated at 800 °C.

4 Conclusion

Carbon-supported NiPc/C catalyst as an novel cathode catalyst for ORR has been successfully prepared by solvent-impregnation along with the high-temperature treatment. A significant influence of the heat-treatment was found on the catalytic activity of NiPc/C catalysts for the ORR. The catalyst heat-treated at 800 °C displayed

significantly improved activity through RDE and CV measurements in oxygen-saturated alkaline electrolyte at room temperature. The number of electrons transferred during the ORR varies with increasing the heat-treatment temperature: 2.23 at 600 °C, 2.15 at 700 °C, 2.93 at 800 °C, and 2.38 at 900 °C. XRD and TEM clearly confirm that the depositions of nanometallic Ni with different sizes are produced with heat-treatment temperature, which are not active for ORR. XPS analysis reveals that both pyridinic-N and graphitic-N should be the active sites responsible for the enhanced ORR activity, at the same time both NiN_4/C and NiN_2/C coexist in the NiPc/C catalysts after the sample was heat-treated at 800 °C.

Here, the catalytic activity of NiPc/C is still low in comparison with reported Co- and Fe-centered phthalocyanines. However, these initial results are promising for the application in alkaline fuel cells. It is believed that by further optimization of the experimental conditions, such as using other synthetic method and modification with metal or nitrogen precursors, both the catalytic activity and the selectivity of NiPc/C could be improved further. We will carry out this research in our next step of study.

Acknowledgments We give our thanks to the financial support from the National Natural Science Foundation of China (21173039), Specialized Research Fund for the Doctoral Program of Higher Education, SRFD (20110075110001), Environmental Protection Engineering Center for Pollution Treatment and Control in Textile Industry, China (20110927) and the Shanghai Leading Academic Discipline Project (B604) Fund.

References

1. Sharma S, Ganguly A, Papalonstantinou P, Miao X, Li M, Hutchison JL, Delichatsios M, Ukleja S (2010) Rapid microwave synthesis of CO tolerant reduced graphene oxide-supported platinum electrocatalysts for oxidation of methanol. J Phys Chem C 114:19459–19466
2. Wang B (2005) Recent development of non-platinum catalysts for oxygen reduction reaction. J Power Sources 152:1–15
3. Wagner N, Schulze N, Gülzow E (2004) Long term investigations of silver cathodes for alkaline fuel cells. J Power Sources 127:264–272
4. Coutanceau C, Demarconnay L, Léger JM (2006) Development of electrocatalysts for solid alkaline fuel cell (SAFC). J Power Sources 156:14–19
5. Zhiani M, Gasteiger HA, Piana M, Catanorchi S (2011) Comparative study between platinum supported on carbon and non-noble metal cathode catalyst in alkaline direct ethanol fuel cell (ADEFC). Int J Hydrogen Energy 36:5110–5116
6. Schulenburg H, Stankov S, Schünemann V, Radnik J, Dorbant I, Fiechter S, Bogdanoff P, Tributsch H (2003) Catalysts for the oxygen reduction from heat-treated iron(III) tetramethoxyphenylporphyrin chloride: structure and stability of active sites. J Phys Chem B 107:9034–9041
7. Jiang L, Hsu A, Chu D, Chen R (2009) Oxygen reduction reaction on carbon supported Pt and Pd in alkaline solutions. J Electrochem Soc 156:B370–B376
8. Gojković SLj, Gupta S, Savinell RF (1999) Heat-treated iron(III) tetramethoxyphenyl porphyrin chloride supported on high-area carbon as an electrocatalyst for oxygen reduction PartII. Kinetics of oxygen reduction. J Electroanal Chem 462:63–72
9. Song C, Zhang L, Zhang J (2006) Reversible one-electron electro-reduction of O_2 to produce a stable superoxide (O_2^-) catalyzed by adsorbed Co(III)hexadecafluoro-phthalocyanine in aqueous alkaline solution. J Electroanal Chem 587:293–298
10. Lefèvre M, Dodelet JP (2003) Fe-based catalysts for the reduction of oxygen in polymer electrolyte membrane fuel cell conditions:determination of the amount of peroxide released during electroreduction and its influence on the stability of the catalysts. Electrochim Acta 48:2749–2760
11. Baker R, Wilkinson DP, Zhang J (2008) Electrocatalytic activity and stability of substituted iron phthalocyanine towards oxygen reduction evaluated at different temperatures. Electrochim Acta 53:6906–6919
12. Lalande G, Tamizhmani G, Côté R, Dignard-Bailey L, Trudeau ML, Schulz R, Guay D, Dodelet JP (1995) Influence of loading on the activity and stability of heat-treated carbon-supported cobalt phthalocyanine electrocatalysts in solid polymer electrolyte fuel cells. J Electrochem Soc 142:1162–1168
13. Faubert G, Lalande G, Côté R, Guay D, Dodelet JP, Weng LT, Bertrand P, Dénès G (1996) Heat-treated iron and cobalt tetraphenylporphyrins adsorbed on carbon black: physical characterization and catalytic properties of these materials for the reduction of oxygen in polymer electrolyte fuel cell. Electrochim Acta 41:1689–1701
14. Lefèvre M, Proietti E, Jaouen F, Dodelet JP (2009) Iron-based catalysts with improved oxygen reduction activity in polymer electrolyte fuel cells. Science 324:71–74
15. Lu Y, Reddy RG (2007) The electrochemical behavior of cobalt phthalocyanine/platinum as methanol-resistant oxygen-reduction electrocatalysts for DMFC. Electrochim Acta 52:2562–2569
16. Kruusenberg I, Matisen L, Shah Q, Kannan AM, Tammeverski K (2012) Non-platinum cathode catalysts for alkaline membrane fuel cells. Int J Hydrogen Energy 37:4406–4412
17. Chen R, Li H, Chu D, Wang G (2009) Unraveling oxygen reduction reaction mechanisms on carbon-supported Fe-phthalocyanine and Co-phthalocyanine catalysts in alkaline solutions. J Phys Chem C 113:20689–20697
18. Bambagioni V, Bianchini C, Filippi J, Lavacchi A, Oberhauser W, Marchionni A, Moneti S, Vizza F, Santo PD, Gallo A, Recchia S, Sordelli L (2011) Single-site and nanosized Fe-Co electrocatalysts for oxygen reduction Synthesis, characterization and catalytic performance. J Power Sources 196:2519–2529
19. Nabae Y, Moriya S, Matsubayashi K, Lyth SM, Malon M, Wu L, Islam NM, Koshigoe Y, Kuroki S, Kakimoto M, Miyata S, Ozaki J (2010) The role of Fe species in the pyrolysis of Fe phthalocyanine and phenolic resin for preparation of carbon-based cathode catalysts. Carbon 48:2613–2624
20. Bezerra CWB, Zhang L, Lee K, Liu H, Marques ALB, Marques EP, Wang H, Zhang J (2008) A review of Fe-N/C and Co-N/C catalysts for the oxygen reduction reaction. Electrochim Acta 53:4937–4951
21. Ozaki J, Tanifuji S, Kimura N, Furuichi A, Oya A (2006) Enhancement of oxygen reduction activity by carbonization Of furan resin in the presence of phthalocyanines. Carbon 44:1324–1326
22. Sehlotho N, Nyokong T (2006) Effects of ring substituents on electrocatalytic activity of manganese phthalocyanines towards the reduction of molecular oxygen. J Electroanal Chem 595: 161–167
23. Ding L, Li Xu, Liu L, Qiao J, Liu Y (2012) Effect of heat-treatment on the activity of nickel phthalocyanine catalysts for oxygen reduction reaction in acid and alkaline electrolytes. Adv Mater Res 535–537:2104–2107

24. Vallejos-Brugos F, Utsumi S, Hattori Y, García X, Gordon AL, Kanoh H, Kaneko K, Radovic LR (2012) Pyrolyzed phthalocyanines as surrogate carbon catalysts: initial insights into oxygen-transfer mechanisms. Fuel 99:106–117
25. Martins Alves MC, Dodelet JP, Guay D, Ladouceur M, Tourillon G (1992) Origin of the electrocatalytic properties for O_2 reduction of some heat-treated polyacrylonitrile and phthalocyanine cobalt compounds adsorbed on carbon black as probed by electrochemistry and X-ray absorption spectroscopy. J Phys Chem 96:10898–10905
26. Bard AJ, Faulkner LR (2000) Electrochemical methods, fundamentals and applications, 2nd edn. Wiley, New York, p 336
27. Ding L, Dai X, Lin R, Wang H, Qiao J (2012) Electrochemical performance of carbon-supported Co-phthalocyanine modified with Co-added metals (M = Fe, Co, Ni, V) for oxygen reduction reaction. J Electrochem Soc 159:577–584
28. He Q, Yang X, He R, Bueno-López A, Miller H, Ren X, Yang W, Koel BE (2012) Electrochemical and spectroscopic study of novel Cu and Fe-based catalysts for oxygen reduction in alkaline media. J Power Sources 213:169–179
29. Kuroki S, Nabae Y, Chokai M, Kakimoto M, Miyata S (2012) Oxygen reduction activity of pyrolyzed polypyrroles studied by ^{15}N solid-state NMR and XPS with principal component analysis. Carbon 50:153–162
30. Van Veen JAR, Colijin HA, Van Baar JF (1988) On the effect of a heat treatment on the structure of carbon-supported metallp-porphyrins and phthalocyanines. Electrochim Acta 33:801–804
31. Wang P, Ma Z, Zhao Z, Jia L (2007) Oxygen reduction on the electrocatalysts based on pyrolyzed non-noble metal/poly-*o*-phenylenediamine/carbon black composites: new insight into the active sites. J Electroanal Chem 611:87–95
32. Velázquez-Palenzuela A, Zhang L, Wang L, Cabot PL, Brillas E, Tsay K, Zhang J (2011) Carbon-supported Fe-Nx catalysts synthesized by pyrolysis of the Fe(II)2,3,5,6-tetra(2-pyridyl)pyrazine complex: structure, electrochemical properties, and oxygen reduction reaction activity. J Phys Chem C 115:12929–12940
33. Liu G, Li X, Ganesan P, Popov NB (2010) Studies of oxygen reduction reaction active sites and stability of nitrogen-modified carbon composite catalysts for PEM fuel cells. Electrochim Acta 55:2853–2858
34. Li X, Liu G, Popov NB (2010) Activity and stability of non-precious metal catalysts for oxygen reduction in acid and alkaline electrolytes. J Power Sources 195:6373–6378
35. Lee K, Zhang L, Liu H, Hui R, Shi Z, Zhang J (2009) Oxygen reduction reaction (ORR) catalyzed by carbon-supported cobalt polypyrrole(Co-PPy/C) electrocatalysts. Electrochim Acta 54:4704–4711
36. Ding L, Qiao J, Dai X, Zhang J, Zhang J, Tian BL (2012) Highly active electrocatalysts for oxygen reduction from carbon-supported copper-phthalocyanine synthesized by high temperature treatment. Int J Hydrogen Energy 37:14103–14113
37. Sidik RA, Anderson BA, Subramanian PN, Kumaraguru PS, Popov NB (2006) O_2 reduction on graphite and nitrogen-doped graphite: experiment and theory. J Phys Chem C 110:1787–1793
38. Lefèvre M, Dodelet JP, Bertand P (2000) O_2 reduction in PEM fuel cells: activity and active site structural information for catalysts obtained by the Pyrolysis at high temperature of Fe precursors. J Phys Chem B 104:11238–11247